CANCER

Lymphangiogenesis-inducing vaccines elicit potent and long-lasting T cell immunity against melanomas

Maria Stella Sasso[1]*†, Nikolaos Mitrousis[1], Yue Wang[1], Priscilla S. Briquez[1], Sylvie Hauert[1], Jun Ishihara[1], Jeffrey A. Hubbell[1], Melody A. Swartz[1,2]*

In melanoma, the induction of lymphatic growth (lymphangiogenesis) has long been correlated with metastasis and poor prognosis, but we recently showed it can synergistically enhance cancer immunotherapy and boost T cell immunity. Here, we develop a translational approach for exploiting this "lymphangiogenic potentiation" of immunotherapy in a cancer vaccine using lethally irradiated tumor cells overexpressing vascular endothelial growth factor C (VEGF-C) and topical adjuvants. Our "VEGFC vax" induced extensive local lymphangiogenesis and promoted stronger T cell activation in both the intradermal vaccine site and draining lymph nodes, resulting in higher frequencies of antigen-specific T cells present systemically than control vaccines. In mouse melanoma models, VEGFC vax elicited potent tumor-specific T cell immunity and provided effective tumor control and long-term immunological memory. Together, these data introduce the potential of lymphangiogenesis induction as a novel immunotherapeutic strategy to consider in cancer vaccine design.

INTRODUCTION

Tumor-associated lymphatics play multifaceted roles in regulating tumor immunity. Our group and others have shown that lymphatic endothelial cells (LECs) can exert direct immunosuppressive functions toward $CD8^+$ T cells by cross-presenting antigens on major histocompatibility complex class I (MHC-I) in the absence of costimulation, as well as by expressing inhibitory ligands and immunosuppressive enzymes and cytokines such as Programmed death-ligand 1 (PDL-1), transforming growth factor–β (TGFβ), inducible nitric oxide synthase (iNOS), and IDO (indoleamine 2,3-dioxygenase) (*1*–*6*). In addition, LECs produce immunomodulatory chemokines that contribute to shaping the tumor microenvironment. Among lymphatic-derived chemokines, C-C motif chemokine ligand 21 (CCL21) attracts $CCR7^+$ leukocytes, including naïve and regulatory T cells as well as dendritic cells (DCs), and is up-regulated in response to tumor-derived vascular endothelial growth factor C (VEGF-C) (*7*); we previously demonstrated that CCL21 in the tumor microenvironment promotes the development of lymphoid-like stromal features that both facilitate DC–T cell interactions and further promote an immunosuppressive microenvironment (*8*).

Despite the immunosuppressive consequences of tumor-associated lymphangiogenesis, lymphatic vessels are critical for adaptive immune responses since they transport immune cells and antigens from the tumor to the draining lymph nodes (dLNs). In the complete absence of dermal lymphatics, melanoma tumors exhibit an impaired antitumor immunity and markedly reduced tumor immune infiltration (*9*). Consistently, the presence of lymphatic markers in human melanomas positively correlates with immune infiltration, including total $CD3^+$ and $CD8^+$ T cells (*9*, *10*), indicating that tumor-associated lymphangiogenesis can promote not only a more immunosuppressive but also a more immune-infiltrated tumor microenvironment. Notably, we found that lymphangiogenic tumors respond far better to immunotherapeutic treatments compared with nonlymphangiogenic counterparts and that this is, at least in part, due to the CCL21-driven evolution of the tumor microenvironment (*11*). Specifically, using mouse melanoma models, we found that the enrichment of tumor-infiltrating naïve T cells before immunotherapy leads to in situ activation postimmunotherapy, which strongly enhances immune-mediated tumor destruction (*11*). Correlative evidence supporting the existence of a "lymphangiogenic potentiation" effect was also seen in patients with human melanoma undergoing immunotherapeutic treatments (*11*). Following up on this finding, Song *et al.* (*12*) recently reported that local administration of VEGF-C in the cerebrospinal fluid (through viral vectors or mRNA therapy) promotes antitumor T cell responses and increases immunotherapy efficacy in mouse models of intracranial glioblastoma.

Thus, the positive correlation between tumor lymphangiogenesis and cancer immunotherapy efficacy suggested to us that lymphangiogenesis-promoting strategies may be promising approaches to improve immunotherapy efficacy in otherwise poorly responsive tumors. However, tumor lymphangiogenesis also plays a well-established role in promoting cancer cell dissemination and metastasis, which severely worsens patient prognosis; the association between tumor-derived lymphangiogenic factors, lymphatic growth or activation, and metastatic spread has been supported by numerous clinical and preclinical studies (*13*). Therefore, therapeutic treatments aimed at directly stimulating lymphangiogenesis within the tumor itself (such as intratumoral administration of VEGF-C) will always be tied to the risk of boosting metastatic dissemination.

Here, we explore an approach to manipulate and exploit lymphatics to promote antitumor immunity that does not involve the direct stimulation of lymphatic vessels within the tumor bed, thereby avoiding the risk of increasing lymphatic-dependent metastases. We developed a lymphangiogenic vaccine that is administered intradermally in a distant site from the tumor but mimics the microenvironment of a lymphangiogenic tumor, using lethally irradiated tumor cells genetically modified to overexpress VEGF-C. When combined with immune adjuvants administered topically in the lymphangiogenic site, these lymphangiogenic vaccines were effective in driving a systemic antitumor immune response in mouse melanoma models. These results demonstrate the potential of lymphangiogenesis induction

[1]Pritzker School for Molecular Engineering, University of Chicago, Chicago, IL, USA. [2]Ben May Department for Cancer Research, University of Chicago, Chicago, IL, USA. *Corresponding author. Email: melodyswartz@uchicago.edu (M.A.S.); mariastella.sasso@psioxus.com (M.S.S.)
†Present address: PsiOxus Therapeutics Ltd., Abingdon, Oxfordshire, UK.

as novel immunotherapeutic strategy, opening up new perspectives in the field of cancer immunotherapy and vaccine design.

RESULTS

Lethally irradiated B16-F10 cells overexpressing VEGF-C induce local lymphangiogenesis, increased lymphatic transport, and naïve T cell infiltration in the cell injection site

We transduced B16-F10 mouse melanoma cells to stably express the model antigen ovalbumin (OVA) and/or VEGF-C, creating four variants: B16-Ctrl (mock transduced), B16-OVA-Ctrl, B16-VEGFC, and B16-OVA-VEGFC. We previously showed that B16-VEGFC and B16-OVA-VEGFC cells, when implanted in syngeneic mice, generate tumors with denser intratumoral and peritumoral lymphatics compared with their respective controls (*2*, *11*). Thus, we first asked whether lethally irradiated B16-VEGFC and B16-OVA-VEGFC cells could also induce lymphangiogenesis in vivo. We first verified that a radiation dose of 50 Gy could completely prevent growth, both in vitro and in vivo, of all four cell lines, indicating the lethality of this dose. We then intradermally injected the lethally irradiated cells in the backs of naïve mice. Eight days after injection, we observed extensive growth of lymphatic vessels within the injection site as assessed by both immunofluorescence imaging on skin tissue sections and flow cytometry on enzymatically digested tissue (Fig. 1, A and B). When examining the kinetics of VEGF-C secretion by the irradiated tumor cells, VEGF-C levels in the skin injection site remained high for the first 3 days after injection and then rapidly decreased over the next 5 days (Fig. 1C), consistent with progressive radiation-induced tumor cell death and consequent loss of the main VEGF-C source. Therefore, this time window of VEGF-C secretion was sufficient to induce the local lymphangiogenesis seen at day 8 (Fig. 1, A and B). In addition, we observed that, at day 8 after cell injection, sites injected with VEGF-C–expressing cells had increased levels of CCL21 (Fig. 1D), a chemokine that recruits $CCR7^+$ cells (including naïve and memory T lymphocytes and DCs) and that is strongly up-regulated in LECs by VEGF-C (*7*, *14*). Consistently, in the injection sites of VEGF-C–overexpressing irradiated B16 cells, we observed enhanced T cell infiltration and an enrichment of both $CD8^+$ and $CD4^+$ naïve T cells compared with central memory (CM) and effector/effector memory (EM) subsets (Fig. 1, E and F).

To validate these findings in a different mouse melanoma model, we generated VEGF-C–overexpressing and control variants from a tumor cell line derived from melanomas growing in $Braf^{V600E}Pten^{-/-}$ genetically modified mice [BP cell line (*15*)]. Similar to what we observed in B16 cells, at day 8 post injection (p.i.), irradiated VEGF-C–overexpressing BP cells induced local lymphatic expansion, enhanced T cell infiltration, and enrichment in the naïve $CD4^+$ T cell compartment compared with control BP cells (fig. S1). However, at day 8, the naïve fractions of both $CD4^+$ and $CD8^+$ subsets were lower than that found in irradiated B16-VEGFC cells at the same time point, and the naïve $CD8^+$ compartment was not enriched compared with controls. This may possibly reflect different kinetics of the evolving cytokine landscape between the two distinct tumor models.

Next, we asked whether the induction of local lymphangiogenesis by lethally irradiated cells led to enhanced lymphatic transport, as we had previously seen with VEGF-C–expressing tumors (*2*). Eight days after irradiated cell inoculation, we injected 0.5-μm fluorescein isothiocyanate (FITC)–labeled microbeads intradermally into the inoculation site, and after 24 hours, we quantified bead uptake by antigen-presenting cells (APCs) in the skin and skin-dLNs. The LN draining lymphangiogenic sites contained markedly higher frequencies of bead-positive APCs compared with control LNs (Fig. 1G). In LN draining lymphangiogenic sites, we observed increased particle accumulation in both migratory DCs ($CD103^+$ DCs and MHC-II^{high} $CD11b^+$ DCs) and LN-resident DC populations ($CD8\alpha^+$ DCs and MHC-II^{low} $CD11b^+$ DC) (*16*). Since 0.5-μm particles are too large for passive drainage into lymphatics (*17*), this suggested that the local activation and expansion of lymphatics induced by the irradiated VEGFC-expressing tumor cells led to increased active particle transport by LECs, which we previously demonstrated could be enhanced by increased fluid drainage (*18*). In addition, the higher particle accumulation within migratory DC subsets in the LNs suggested an improved APC trafficking from the skin of lymphangiogenic sites to the dLNs. The total frequencies of APCs in the dLNs and cell injection sites were instead similar between Ctrl and VEGF-C groups for most of the APC subsets considered (Fig. 1H).

VEGF-C overexpression in irradiated tumor cell vaccines promotes T cell priming both in the vaccine injection site and in the dLNs

Because naïve T cells were enriched in the injection sites of irradiated VEGF-C–expressing tumor cells, we asked whether these T cells could undergo in situ priming and proliferation in the presence of the appropriate stimuli. To investigate this, we used the adjuvant imiquimod (IMQ), a TLR7 agonist, as a cream formulation topically applied on the injection site of irradiated B16-OVA-Ctrl and B16-OVA-VEGFC cells to create vaccines (Ctrl vax and VEGFC vax, respectively). Seven days later (Fig. 2A), mice received an adoptive transfer of naïve $CD8^+$ T cells isolated from OT-1 and pmel transgenic mice, which recognize immunodominant MHC-I–restricted epitopes for OVA and the gp100 melanoma antigen, respectively. These transferred $CD8^+$ T cells were labeled with carboxyfluorescein diacetate succinimidyl ester (CFSE) or CellTrace to determine proliferation (as assessed by dye dilution) and could be further tracked by their congenic markers. Also, starting from the day of adoptive transfer, mice received daily injections of FTY720 (FTY), which blocks S1P receptors and thus prevents the egress of both naïve and effector T cells from lymph nodes (*19*, *20*).

The efficacy of FTY was verified by a marked drop in the frequencies of circulating activated (proliferated) $CD8^+$ T cells detected in the blood (Fig. 2B), as a consequence of their sequestering in the sites of initial activation. In the vaccine-draining LNs (vax-dLNs) of both the Ctrl and VEGFC vax groups, we measured overall high numbers of activated OT-1 and pmel $CD8^+$ T cells, both with and without FTY (Fig. 2C). In the absence of FTY, increased numbers of activated OT-1 and pmel $CD8^+$ T cells were found in VEGFC vax-dLNs compared with Ctrl vax-dLNs, indicating an overall enhanced T cell activation with VEGF-C vaccination (Fig. 2C). However, while the frequencies of activated OT-1 T cells tended to increase in Ctrl vax-dLNs following FTY administration and effector T cell entrapment in LNs, this was not observed for VEGFC vax-dLNs, where those frequencies remained approximately constant (Fig. 2C). This suggested that the higher frequencies of activated T cells seen in the VEGFC vax-dLNs versus Ctrl vax-dLNs in the absence of FTY were not due only to an enhanced priming within the dLNs.

In VEGFC vax injection sites in the skin, we found high levels of activated OT-1 and pmel $CD8^+$ T cells both in the absence and presence of FTY treatment (Fig. 2, D and E). In contrast, Ctrl vax sites

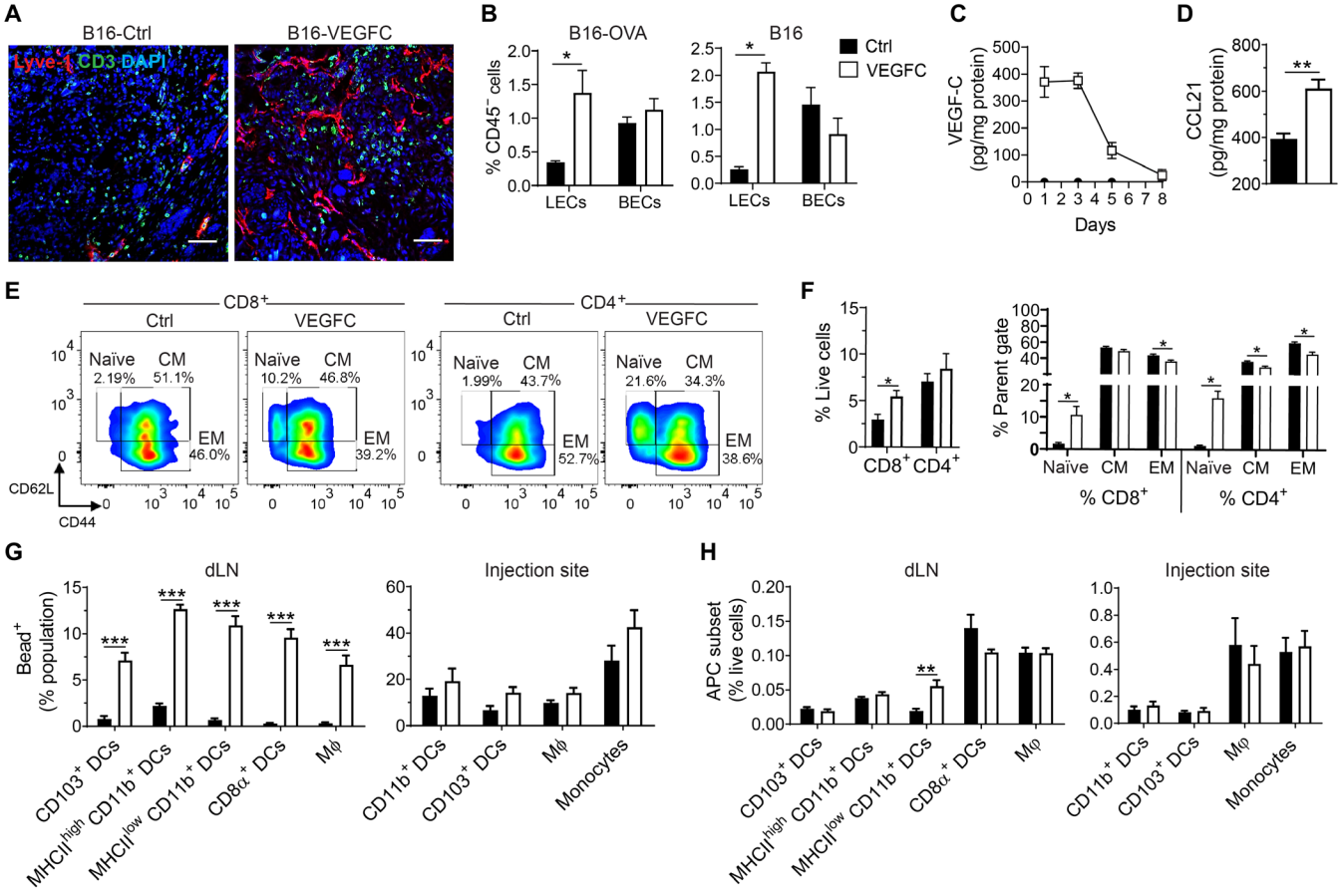

Fig. 1. Irradiated VEGF-C–overexpressing tumor cells induce local lymphangiogenesis, naïve T cell infiltration, and enhanced lymphatic transport to the dLNs. (**A** to **F**) Lethally irradiated B16-Ctrl or B16-VEGFC cells, either OVA-expressing or not, were injected intradermally, and the skin from the injection sites was analyzed 8 days later. (A) Representative images of skin sections immunostained for Lyve-1 (lymphatic vessels, red), CD3 (T cells, green), and 4′,6-diamidino-2-phenylindole (DAPI) (nuclei, blue). Scale bars, 50 μm. (B) Flow cytometry–based quantification of lymphatic and blood endothelial cells (LECs and BECs). (C) VEGF-C concentration over time by enzyme-linked immunosorbent assay (ELISA). (D) CCL21 concentration at day 8 by ELISA. (E) Representative flow cytometry plots of T cell subsets, gated on total $CD8^+$ or $CD4^+$ T cells. (F) Frequencies of total $CD8^+$ and $CD4^+$ T cells (left) and relative fractions of subsets: naïve = $CD62L^+$ $CD44^-$, CM (central memory) = $CD62L^+$ $CD44^+$, EM (effector and effector memory) = $CD62L^-$ $CD44^+$. (**G** and **H**) Seven days after irradiated tumor cell injection, 0.5-μm fluorescein isothiocyanate–labeled beads were injected intradermally in the same spot and, after 24 hours, injection sites and dLNs were analyzed by flow cytometry. (G) Percentages of bead-positive cells within each indicated antigen-presenting cell (APC) subset. (H) Frequencies of APC subsets in the dLNs and injection sites. Legend in (B) applies to the whole figure. All experiments were done in duplicate with $n = 4$ each. Values are reported as means ± SEM. $^*P < 0.05$, $^{**}P < 0.01$, and $^{***}P < 0.001$ using a two-tailed Student's t test.

contained very low numbers of these cells, which almost completely disappeared with FTY administration (Fig.2, D and E). Because activated OT-1 and pmel $CD8^+$ T cells were abundantly found in the VEGFC vax injection sites even when depleted from the blood circulation through FTY treatment, we reasoned that this excluded a mere recruitment of circulating effectors into the vax site and pointed instead to an in situ activation mechanism. This could be further illustrated by comparing ratios of activated T cells in the injection site versus dLN, where VEGFC vax was significantly higher than Ctrl vax (Fig. 2F). Thus, transferred $CD8^+$ T cells were activated in situ in the vaccine injection site and in the dLNs with VEGFC vax, but only in the dLNs in Ctrl vax, leading to an overall stronger T cell activation with VEGF-C vaccination.

Lymphangiogenic vaccines elicit a strong melanoma-specific T cell immunity

Next, we sought to determine the extent to which lymphangiogenic vaccines could be used to induce endogenous T cell responses directed against melanoma antigens. To investigate this, we developed vaccines containing irradiated B16-VEGFC and B16-Ctrl cells, which constitute a less immunogenic and thus more translationally relevant model compared with OVA-expressing cell lines. As adjuvants, we combined IMQ cream applications with an intradermal injection of a low dose of anti-CD40 agonist antibodies, both administered topically at the site of irradiated cell injection. Anti-CD40 agonist antibodies activate the CD40 receptor expressed on APCs, inducing their maturation and effective antigen presentation. Since, as discussed above, part of the mechanism of action of lymphangiogenic vaccines is promoting in situ antigen presentation and T cell activation, we reasoned that the synergy between lymphangiogenesis and immune activation could be increased by using locally retained immune adjuvants. To this end, in this study, we used an engineered variant of the anti-CD40 antibody containing a peptide domain derived from placenta growth factor–2 that binds to the extracellular matrix and prolongs antibody retention in the injection site compared with the native antibody form

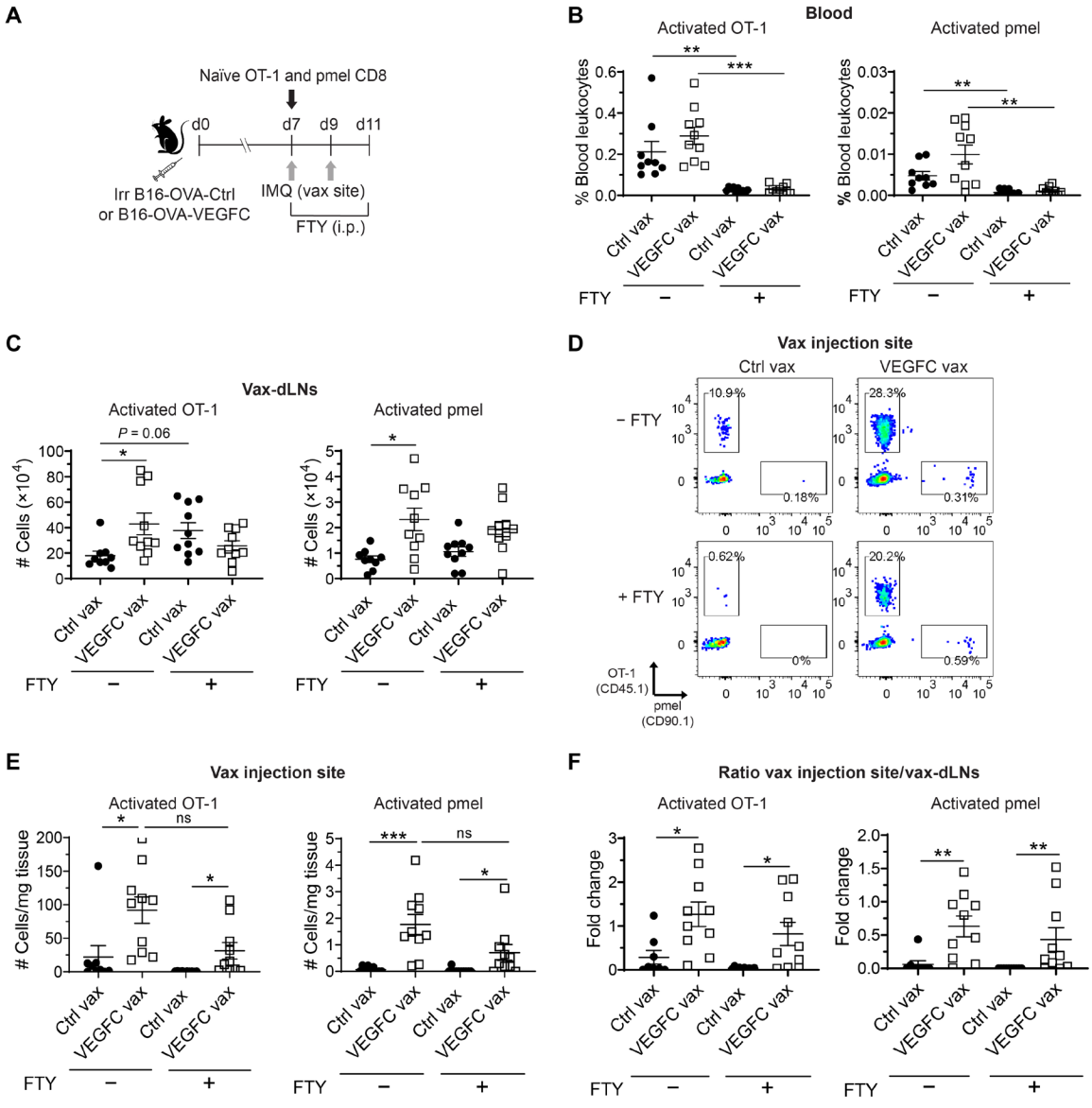

Fig. 2. Naïve T cells can be activated in situ in VEGFC vax injection sites. (**A**) Experimental design: Irradiated (irr) B16-OVA-Ctrl or B16-OVA-VEGFC cells were injected intradermally into the back skin, and IMQ was applied on the injection site 7 and 9 days later. On day 7, mice received an adoptive transfer of naïve CD8$^+$ T cells isolated from OT-1 and pmel transgenic mice, labeled with either CFSE or CellTrace fluorescent dyes, and daily administration of FTY720 [intraperitoneally (i.p.)] was started on the same day. Mice were euthanized on day 11 for analysis. (**B** and **C**) Activated (proliferated) OT-1 and pmel CD8$^+$ T cells in the (B) blood (as % CD45$^+$ cells) and (C) dLNs (as total numbers). (**D**) Representative flow cytometry plots for OT-1 and pmel CD8$^+$ T cells in the injection sites after gating on total CD8$^+$ T cells. (**E**) Numbers of activated OT-1 and pmel CD8$^+$ T cells in the vaccine injection site. (**F**) Ratios of activated OT-1 and pmel CD8$^+$ T cells (expressed as % of total CD8$^+$ T cells) in vaccine injection sites versus draining LNs. Pooled data from two independent experiments ($n = 9$ to 10). Data are reported as means ± SE. *$P < 0.05$, **$P < 0.01$, and ***$P < 0.001$ using Kruskal-Wallis with Dunn's posttest. ns, not significant.

(PlGF-2$_{123–144}$ matrix-binding anti-CD40 antibody, here referred to as MB-αCD40) (*21*).

Mice were immunized with irradiated B16-Ctrl or B16-VEGFC cells together with IMQ and MB-αCD40 (Fig. 3A), and after 17 days, splenocytes from immunized animals were isolated and restimulated ex vivo with an immunodominant MHC-I–restricted epitope from the Trp2 mouse melanoma antigen (Trp2$_{180–188}$, SVYDFFVWL). VEGFC vax induced a stronger Trp2-specific CD8$^+$ T cell response compared with mice treated with Ctrl vax, as determined by interferon-γ (IFN-γ) production (Fig. 3, B and C). Baseline (unstimulated) levels of both IFN-γ and interleukin-2 (IL-2) were higher in VEGFC vax–treated mice compared with control vaccinated mice (Fig. 3C), suggesting overall enhanced basal levels of T cell activation associated with VEGFC vax.

To confirm that the increased immunogenicity of VEGFC vax over Ctrl vax was specifically due to VEGF-C signaling and subsequent lymphangiogenesis, and exclude potential biases related to the use of two distinct cell lines for vaccination, we immunized mice with VEGFC vax and administered mF4-31C1, a blocking antibody against VEGFR-3 (*11*). This prevented the lymphangiogenesis that

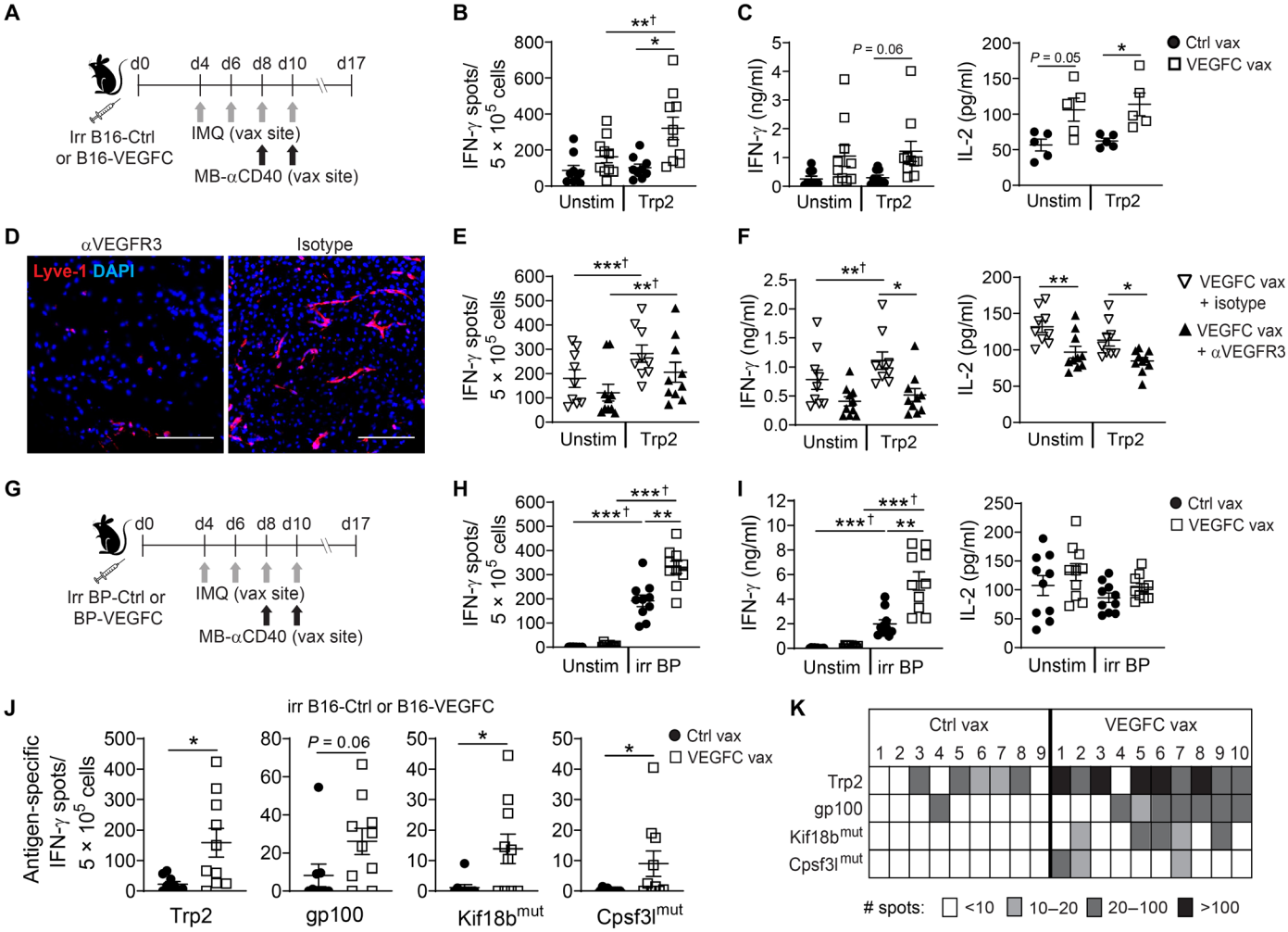

Fig. 3. VEGF-C–driven lymphangiogenesis boosts vaccine-induced T cell immunity. (**A**) Schematic of the immunization protocol. Irradiated B16-Ctrl or B16-VEGFC cells were injected intradermally on day 0 (d0). On days 4, 6, 8, and 10, IMQ was applied onto the skin, and on days 8 and 10, MB-αCD40 was injected intradermally, both at the cell injection site. Mice were euthanized at day 17, and splenocytes were restimulated ex vivo against the indicated antigens. (**B**) Frequencies of IFN-γ–producing splenocytes measured by ELISPOT. (**C**) IFN-γ and IL-2 secretion measured by ELISA. (**D** to **F**) Mice were immunized with VEGFC vax as shown in (A) but also received intraperitoneal injections of mF4-31C1 (αVEGFR-3) or control immunoglobulin G antibodies every 3 to 4 days. (D) Representative images of skin sections at day 17 immunostained for Lyve-1 (red) and DAPI (blue). Scale bars, 50 μm. (E) Frequencies of IFN-γ–producing splenocytes measured by ELISPOT. (F) IFN-γ and IL-2 secretion measured by ELISA. (**G** to **I**) Mice were immunized as in (A) but with irr BP-Ctrl or BP-VEGFC cells rather than B16. (G) Schematic of the immunization protocol. (H) Frequencies of IFN-γ–producing splenocytes measured by ELISPOT. (I) ELISA quantification of IFN-γ and IL-2 secretion. (**J** and **K**) Mice were immunized as in (A), and ex vivo T cell reactivity was tested against four different melanoma-associated peptides at day 17. (L) Frequencies of antigen-specific IFN-γ–producing T cells (after subtracting unstimulated control wells) by ELISPOT. (M) Breadth of reactivity against each antigen for each individual mouse expressed as number of antigen-specific IFN-γ spots. Data from one of two repeated experiments, shown as means ± SE. $^{*}P < 0.05$, $^{**}P < 0.01$, and $^{***}P < 0.001$ by Welch's analysis of variance (ANOVA) with Dunnett's T3 posttest (B, H, and I), one-way ANOVA with Tukey's posttest (C, E, and F), Mann Whitney test (J), or †paired Student's *t* test.

was seen in untreated (Fig. 1, A and B) and isotype control immunoglobulin G (IgG)–treated mice (Fig. 3D). In addition, VEGFR-3 blockade reduced both Trp-2–specific IFN-γ production and basal levels of IL-2 in the spleen, as assessed by ex vivo antigen stimulation of splenocytes at day 17 from immunization (Fig. 3, E and F). These data confirmed that the superior efficacy of VEGFC vax was dependent on VEGFR-3 signaling.

To validate VEGFC vax immunogenicity in a different melanoma cell line, we immunized mice with irradiated BP-Ctrl or BP-VEGFC cells together with IMQ and MB-αCD40, using the same immunization protocol as before (Fig. 3, G to I). Unlike B16 cells, BP cells do not express detectable levels of melanoma-associated antigens such as Trp2, Trp1, and gp100 (fig. S2A). Therefore, we measured vaccine-induced immune reactivity directed against whole irradiated BP cells, allowing us to account for immune responses mounted against unknown tumor antigens, including potential antigens originated through unique mutations present in this cell line. Splenocytes and LN cells from VEGFC vax–immunized mice showed stronger reactivity against BP cells compared with the Ctrl vax–immunized group, as assessed by IFN-γ production (Fig. 3, H and I, and fig. S2, B to D). In contrast, very low levels of cytokine production were induced by Trp2 and gp100 peptides (fig. S2, B to D), consistent with the lack of expression of these antigens in the BP cell line. Notably, in this model, we did not observe an increase in baseline IL-2 production

in VEGFC vax versus Ctrl vax, as seen for B16 cell–based vaccines. Because IFN-γ is known to be abundantly secreted by both $CD8^+$ T cells and T helper cell 1–switched $CD4^+$ T cells, while IL-2 is predominantly a $CD4^+$ T cell–derived cytokine (*22*, *23*), the observed differences in IFN-γ secretion in the absence of equivalent changes in IL-2 levels might be indicative of a CD8-dominated immune response in the BP model. This, in turn, might be related to a prevalence of CD8-resticted immunogenic epitopes in this cell line.

Having established that VEGFC vax elicits a stronger T cell response than Ctrl vax against either an immunodominant antigen such as Trp2 or whole BP tumor cells, we sought to determine whether VEGFC vax could activate a broader repertoire of T cells targeting multiple distinct antigens, which can be advantageous for cancer vaccination. To investigate this, we immunized mice with B16-based VEGFC vax or Ctrl vax as before (Fig. 3A) and assessed ex vivo immune reactivity against three additional B16 antigens: namely, the MHC-I–restricted short peptide from gp100 melanoma protein $hgp100_{25–33}$ (KVPRNQDWL), as well as long peptides from two known B16 mutated neoantigens ($Kif18b^{mut}$ and $Cpsf3l^{mut}$), which can result in both MHC-I and MHC-II antigen presentation (*24*). For each of the antigens considered, mice immunized with VEGFC vax had higher frequencies of IFN-γ–producing antigen-specific T cells compared with control vaccinated mice (Fig. 3J). When considering all antigens together, mice receiving VEGFC vax appeared to have mounted a broader T cell immunity, because they developed a detectable reactivity against a higher number of different antigens compared with mice in the Ctrl vax group (Fig. 3K).

Lymphangiogenic vaccines provide complete prophylactic protection against B16 melanoma and delay the growth of preexistent tumors

Since VEGFC vax induced a strong and broad antigen-specific T cell response in naïve mice, we next asked whether this was sufficient to protect immunized animals from subsequent tumor challenge in a distant site. First, we verified that irradiated VEGF-C–overexpressing tumor cells, injected into one side of the back skin, did not induce lymphangiogenesis in distant tumors implanted in the other side (fig. S3). This was important to ensure that any effects on the distant tumors were due to changes only in the vaccine site. Furthermore, the absence of lymphangiogenesis in distant tumors likely excluded any potential effects of VEGFC vax in promoting lymphatic metastasis.

To provide a comparison with another cell-based cancer vaccine platform already in clinical trials, we used irradiated B16-F10 transduced to overexpress granulocyte-macrophage colony-stimulating factor (B16-GM-CSF). This approach, known as GM-CSF Vaccine (GVAX), has been shown to be effective either alone or in combination with checkpoint blockade in the B16 melanoma model (*25*–*27*) and in other mouse tumor models (*28*). In clinical trials, GVAX was demonstrated to be safe and able to induce a tumor-specific immune response (although with limited clinical efficacy) in multiple human cancer types (*29*–*33*). First, we compared the immune infiltrate 8 days after injection of irradiated B16-GM-CSF versus irradiated B16-VEGFC and found distinct patterns of myeloid cell and T cell infiltration in the skin injection site. Specifically, irradiated B16-GM-CSF cells recruited more myeloid $CD11b^+$ DCs and $CD4^+$ T cells, while irradiated B16-VEGFC cells drove a stronger infiltration of $CD8\alpha^+$ cross-presenting DCs and $CD8^+$ T cells (fig. S4). Furthermore, irradiated B16-VEGFC recruited more naïve T cells. When both cell types were coinjected together, we saw similar recruitment of total $CD8^+$ T cells, naïve $CD8^+$, and naïve $CD4^+$ T cells as with the B16-VEGFC only group, and similar recruitment of total $CD4^+$ T cells as in the B16-GM-CSF only group (fig. S4).

We prophylactically vaccinated naïve mice with Ctrl vax, VEGFC vax, or GVAX and 17 days following immunization, we inoculated them with unmodified (nonirradiated) B16-F10 cells on the contralateral side (Fig. 4, A to E). Animals in the GVAX treatment group received irradiated B16-GM-CSF only, without addition of IMQ and MB-αCD40, since GM-CSF itself acts as immune adjuvant by recruiting DCs and inducing their maturation (*34*). Immunization with VEGFC vax resulted in substantially higher frequencies of circulating Trp2-specifc $CD8^+$ T cells compared with the other groups (Fig. 4B) and, notably, led to complete prevention of tumor growth in 100% of the mice (Fig. 4, C and D). In contrast, Ctrl vax and GVAX both provided a partial protection against B16 tumor challenge, with roughly half of the mice rejecting the tumor inoculum, while the remaining animals developed tumor masses and ultimately reached end point tumor size (Fig. 4, C and D).

To assess long-term immunological memory, about 10 months (320 days) following the initial vaccination, all mice that had survived the first tumor injection were rechallenged with B16 tumors on the same site as the first injection (Fig. 4A). Mice that had initially received VEGFC vax showed the strongest memory response, with 50% of the mice surviving the second tumor challenge (Fig. 4E), indicating that lymphangiogenic vaccination also provided an effective long-term protective immunity.

Having observed a markedly increased efficacy of VEGFC vax over GVAX, we further asked whether this was specifically due to VEGF-C–mediated modulation of vaccine-induced immunity rather than to the additive effects of VEGF-C plus topical immune adjuvants. To clarify this point, we compared prophylactic VEGFC vax to either conventional GVAX (composed of irradiated B16-GM-CSF only) or GVAX plus local administration of IMQ and MB-αCD40 at the same dosage and schedule as for VEGFC vax. Notably, we found that even when GVAX was further adjuvanted by the addition of IMQ and MB-αCD40, it remained less effective than VEGFC vax, in terms of its ability to both prevent tumor growth and to elicit systemic expansion of Trp2-specifc $CD8^+$ T cells (Fig. 4, F to H). These data further highlight the unique immunomodulatory effects of VEGF-C versus GM-CSF in synergizing with APC-activating immune adjuvants and shaping vaccine-induced adaptive immunity. None of these vaccine formulations induced detectable hepatic, pancreatic, kidney, or cardiac toxicity, as assessed by measurement of serum markers commonly used for the monitoring of immunotherapy-related adverse events (fig. S5) (*35*).

Last, we evaluated the efficacy of VEGFC vax in a therapeutic setting, after the tumors had already been implanted (Fig. 5A). Because of the fast growth rate and poor immunogenicity of the B16 melanoma model, we combined systemic administration of anti-PD-1 antibodies (αPD-1) with VEGF-C vaccination, resulting in a significantly delayed tumor growth and prolonged mouse survival compared with both untreated mice and mice treated with Ctrl vax + αPD-1 (Fig. 5, B to D). Notably, in these studies, we did not observe formation of metastases in any of the experimental groups in either tumor-draining LNs, distant organs (such as lung and liver), or the contralateral vaccine injection site, further confirming that VEGFC vax, implanted remotely from the primary tumor, does not increase the risk of metastasis formation. Overall, these data indicate that lymphangiogenic vaccination shows promise as a therapeutic approach

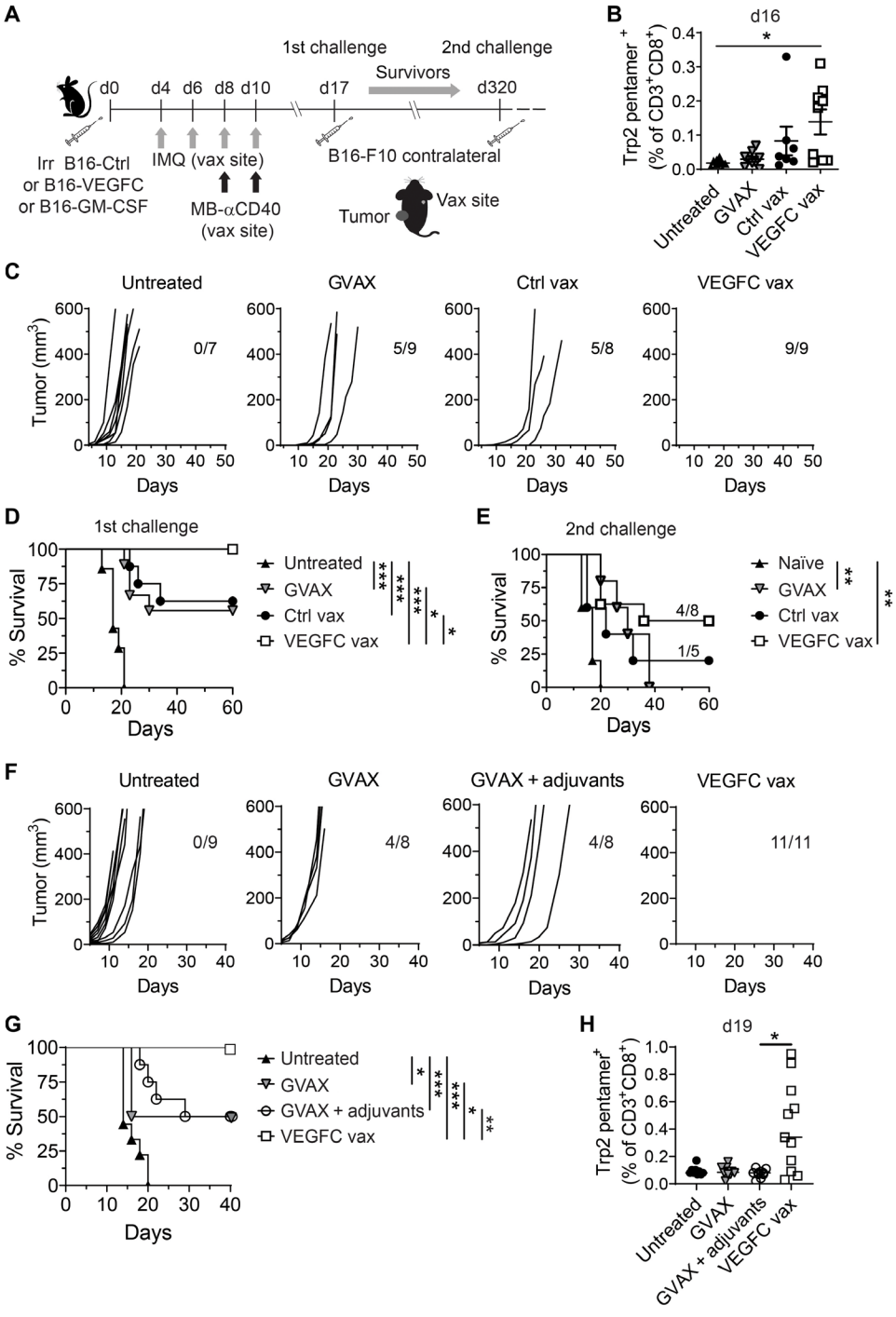

Fig. 4. VEGFC vax provides complete protection against melanoma challenge and long-term immunological memory. (**A**) Experimental design. Mice were vaccinated intradermally with Ctrl Vax, VEGFC vax, or GVAX over the right shoulder, and on day 17, B16-F10 cells were injected intradermally on the contralateral side. Ctrl vax and VEGFC vax were composed of irradiated tumor cells (B16-Ctrl or B16-VEGFC) plus IMQ and MB-αCD40, while GVAX consisted of irradiated GM-CSF–overexpressing B16-F10 without additional immune adjuvants. Tumor growth was recorded, and mice that rejected tumors were rechallenged 320 days later with B16-F10 cells intradermally. (**B**) Frequencies of circulating Trp2-specific $CD8^+$ T cells at day 16 assessed by pentamer staining. (**C**) Individual tumor growth curves showing ratios of mice with complete tumor rejection following the first challenge. (**D** and **E**) Survival curves following the (D) first and (E) second tumor challenges. In (E) naïve mice were used as positive controls for tumor growth. (**F** to **H**) The above experiment was repeated (without second challenge) to further compare GVAX supplemented with IMQ and MB-αCD40 (GVAX + adjuvants) against VEGFC vax. (F) Individual tumor growth curves and ratios of mice with complete tumor rejection. (G) Survival curves. (H) Frequencies of circulating Trp2-specific $CD8^+$ T cells at day 19. Data shown are from (B to E) one of two repeated experiments or (F to H) one experiment, $n = 7$ to 11 mice per group. $^*P < 0.05$, $^{**}P < 0.01$, and $^{***}P < 0.001$ using Kruskal-Wallis with Dunn's posttest (B and H) or log-rank test (D, E, and G).

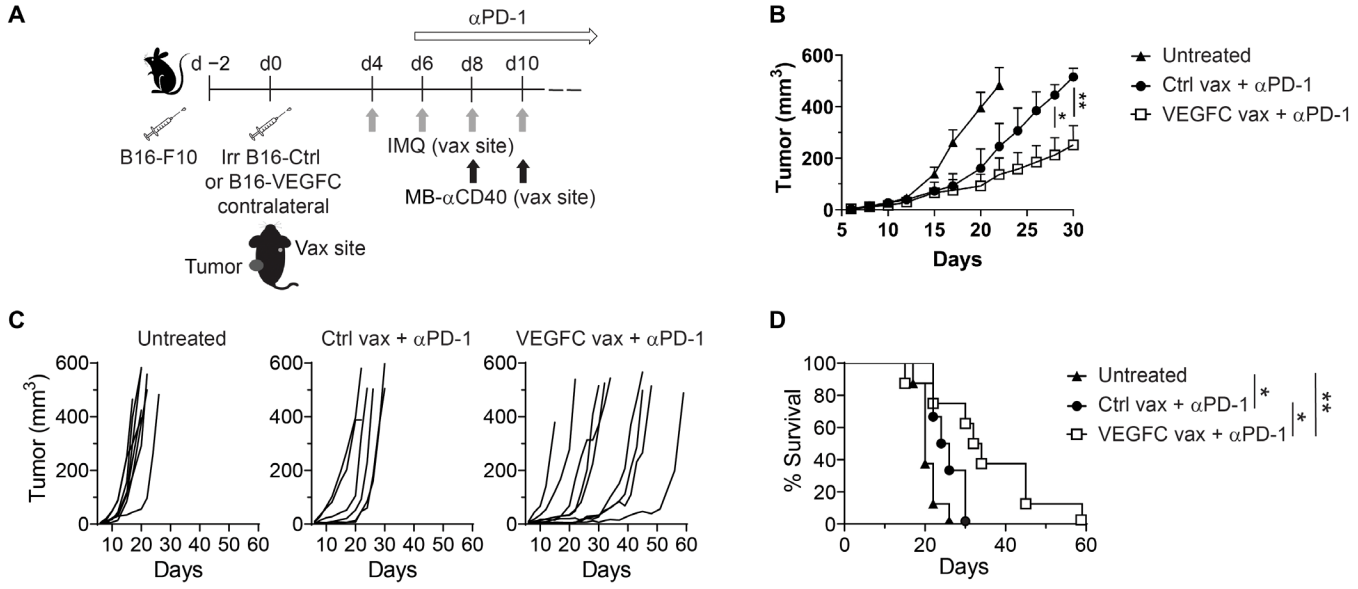

Fig. 5. VEGFC vax combined with PD-1 blockade delays the growth of preexistent B16 melanomas. (**A**) Treatment schedule: Mice were inoculated intradermally with B16-F10 tumor cells and then therapeutically vaccinated on the contralateral side with VEGFC vax or Ctrl vax according to the protocol described, starting 2 days following tumor injection. αPD-1 blocking antibodies were administered intraperitoneally every 3 to 4 days starting from day 6, for a total of four injections. (**B**) Average tumor growth curves (means ± SEM). (**C**) Individual tumor growth curves. (**D**) Survival curves. Shown are representative data from one of two repeated experiments with $n = 7$ to 9 mice per group. $^{*}P < 0.05$ and $^{**}P < 0.01$ using (B) two-way ANOVA with Sidak's multiple comparisons test or (D) log-rank test.

for the treatment of melanoma, particularly in combination with antibody checkpoint blockade therapy.

DISCUSSION

In this study, we introduce a new potential strategy for cancer immunotherapy. Following our demonstration in melanoma that lymphangiogenic tumors—despite being more metastatic—are more responsive to immunotherapy (*11*), we sought to develop a translational strategy that could exploit the lymphangiogenic potentiation of immune responses while avoiding the prometastatic aspects of tumor lymphangiogenesis. Using lymphangiogenic vaccines composed of lethally irradiated VEGF-C–overexpressing melanoma cells and a combination of topical immune adjuvants (VEGFC vax), we demonstrated that VEGF-C–induced lymphangiogenesis boosts vaccine efficacy by at least two different mechanisms (summarized in Fig. 6). First, more abundant and enlarged lymphatic vessels at the site of vaccine injection mediate increased lymphatic transport to vax-dLNs (Fig. 1G), leading to more activation there, as evidenced by the higher numbers of activated antigen-specific $CD8^+$ T cells found in LN draining VEGFC vax injection sites compared with those draining Ctrl vax sites (Fig. 2C). Second, intradermal lymphangiogenic vaccine sites recruit more naïve T cells, due to locally increased levels of CCL21 (Fig. 1, D to F), leading to in situ activation directly within the vaccine site (Fig. 2, D to F).

Consistently with the notion of enhanced activation, we demonstrated that lymphangiogenic vaccines elicit a broad T cell immunity targeting multiple mouse melanoma antigens. In the B16 model, the T cell response directed against the Trp2 melanoma–associated protein appeared to be dominant; however, we also found that VEGFC vax induced stronger immunoreactivity against the gp100 tissue–associated antigen and against two known B16 mutated neoantigens [$Kif18b^{mut}$ and $Cpsf3l^{mut,}$ (*24*)] compared with Ctrl vax. The generation of a broad-spectrum antigen-specific immunity is advantageous in cancer vaccination since it minimizes the risk to select resistant tumor subclones that do not express the targeted antigen (*36*). It has also been shown in the B16 model that peptide vaccines targeting multiple antigens simultaneously are more effective than vaccines containing only one or two different antigens (*37*). Vaccines composed of whole-tumor cells may be particularly suited to induce a multispecific tumor immunity, since they potentially contain a broad range of different tumor antigens and do not require their molecular identification.

The VEGFC vax approach characterized in this study was based on the use of genetically engineered melanoma cell lines. Irradiated, genetically engineered cell lines have been used to formulate allogeneic cell–based vaccines for different human cancers, including melanoma (*38*), prostate, and pancreatic cancer (*33*, *39*). Cell line–based vaccines rely on the presence of shared antigens expressed in tumors with same histological origin. In human melanoma, multiple melanocyte-associated proteins (among which Melan-A/MART-1, gp100, and tyrosinase) are able to elicit a $CD8^+$ T cell immunity and are expressed in tumors from different patients and in normal melanocytes, making this cancer type a suitable candidate for cell line–based vaccination (*40*, *41*). Cellular vaccines can alternatively be formulated using tumor cells directly obtained from resected tumor samples to generate an autologous vaccine. Studies with GVAX have shown that vaccination with irradiated autologous tumor cells [either transduced ex vivo with viral vectors to overexpress GM-CSF (*29*, *30*) or mixed with bystander GM-CSF–overexpressing cell lines (*31*, *32*)] is a safe and feasible approach in the clinical practice. Although autologous vaccines may be more challenging to produce compared with allogenic approaches, the use of patient-derived tumor cells allows for a potentially more relevant anticancer immune response that includes patient-specific mutated antigens. The lessons learned from the extensive clinical experience with GVAX could potentially guide the

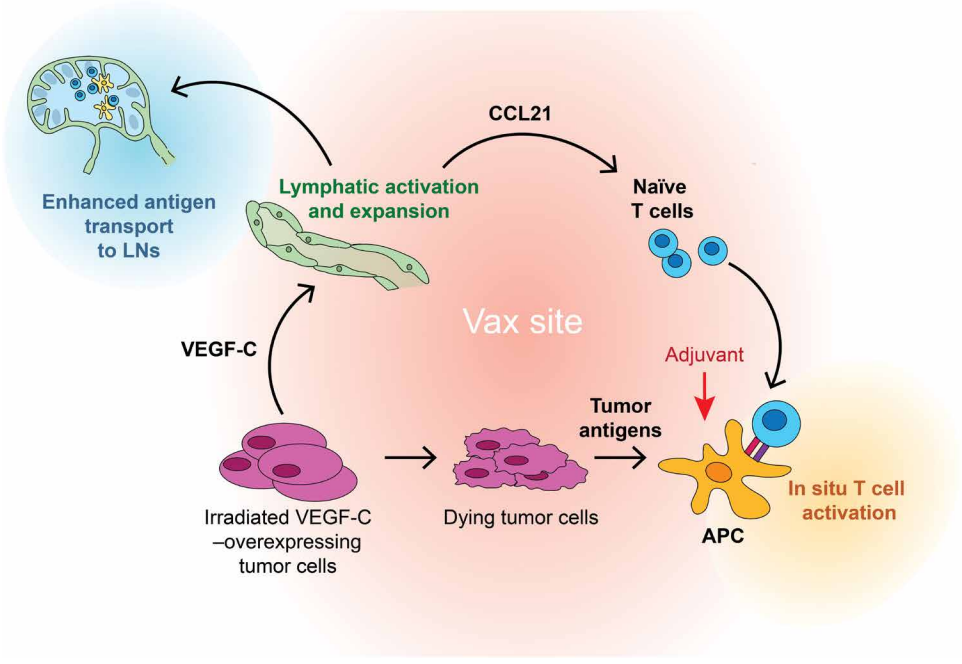

Fig. 6. Proposed model for VEGFC vax mechanism of action. Lethally irradiated tumor cells, injected intradermally, undergo radiation-induced cell death and provide a source of tumor-associated antigens. When transduced to overexpress VEGF-C, these irradiated cells also activate local lymphatics to undergo proliferation and increase antigen transport to the dLNs. In addition, VEGF-C stimulates lymphatics to secrete increased levels of chemokines that modulate the immune infiltrate in the vaccine site, particularly CCL21, which recruits naïve T cells and APCs. Later, when immune adjuvants are locally administered, APCs are further recruited to the vaccine site and activated, allowing presentation of tumor cell–derived antigens to T cells and in situ priming. Together with enhanced LN priming due to increased antigen transport, this supports a more robust and long-lasting antitumor immune response.

clinical translation of VEGFC vax, for which both allogenic and autologous vaccination strategies could be envisioned. Our data indicate an enhanced potency of VEGFC vax over GVAX in preclinical models, due to its different mechanisms of action.

A major advantage of lymphangiogenic vaccines over tumor-targeting prolymphangiogenic approaches is that vaccines can be administered in a remote location from the tumor. Since our discovery that lymphangiogenic melanomas are more responsive to immunotherapy, we have explored multiple ways to exploit this therapeutically, including directly inducing lymphangiogenesis in uninflamed, "cold" melanoma models (unpublished). However, the obvious risk with this latter approach is the possibility of enhancing metastasis, since there is a well-established correlation in melanoma and other cancers between lymphangiogenesis and presence of LN metastasis (*13*, *42*). Lymphangiogenic vaccines allow to completely avoid this potential risk.

Furthermore, in contrast to tumor-targeting approaches, vaccination does not require the presence of an accessible tumor site for injection and therefore can be administered (i) for the therapy of cancers with poor accessibility, and (ii) as an adjuvant treatment following surgical resection of primary tumors, to treat potential nonclinically detectable residual disease and prevent relapse. Administration of cellular vaccines in an adjuvant setting has been investigated in patients with melanoma considered at high risk of relapse based on the clinicopathologic characteristics of their tumors and was shown to be feasible and well tolerated (*38*, *43*). Adjuvant treatments for resectable melanoma with satisfactory toxicity and efficacy profiles are still lacking (*44*), and lymphangiogenic vaccines may be a promising candidate therapeutic option for this application. Last, lymphangiogenic vaccines may be used to treat distant metastases in advanced cancers. Although we did not explore the efficacy of VEGFC vax on treating metastatic tumors in this study, it will be important to perform these studies in future work.

In summary, this study introduces the previously unexplored concept that VEGF-C stimulation can be used to induce local lymphangiogenesis and boost vaccine-induced tumor-specific immunity, opening new perspectives for the design of efficient anticancer vaccines. In addition, it highlights the potential of lymphangiogenic vaccines for the specific purpose of inducing immunity against a broader repertoire of tumor antigens, in contrast to other cancer vaccines. Lymphangiogenic cell–based vaccines induce a potent tumor-specific T cell immunity directed against mouse melanoma antigens and have potential for clinical translation.

MATERIALS AND METHODS

Experimental design

The aim of this study was to investigate whether the newly described positive synergy between lymphangiogenesis and cancer immunotherapy could be exploited in a cancer vaccine. To this end, we first demonstrated that lethally irradiated, VEGF-C–overexpressing melanoma cells could induce local lymphangiogenesis and attract lymphocytes after intradermal injection. Then, we developed a vaccine using these cells with locally applied adjuvants, namely, IMQ and an engineered variant of an agonistic anti-CD40 antibody that binds to extracellular matrix components for enhanced local retention (*21*). We evaluated the immunogenicity of VEGFC vax in healthy mice as compared with a nonlymphangiogenic vaccine with equivalent

composition (Ctrl vax), using cell lines derived from either B16-F10 or BP melanomas. Vaccine-induced immunity was evaluated by ex vivo stimulation of spleen and lymph nodes cells with tumor antigens and measurement of cytokine production, and by in vivo tracking of proliferation of antigen-specific $CD8^+$ T cells. Last, superior antitumor efficacy of VEGFC vax was determined in the B16 melanoma model in both prophylactic and therapeutic vaccination schedules, the latter in combination with anti–PD-1 antibodies.

Mice

Female C57BL/6 mice (the Jackson laboratory) were used between 8 and 12 weeks of age. OT-I CD45.1.2 mice, generated from crossing CD45.1 mice (B6.SJL-$Ptprc^a Pepc^b$/BoyJ) and OT-I mice [C57BL/6 Tg(TcraTcrb)1100Mjb/J], and Pmel mice [B6.Cg-$Thy1^a$/Cy Tg(TcraTcrb) 8Rest/J], all from the Jackson laboratory, were used at 8 to 12 weeks old as sources of TCR-transgenic $CD8^+$ T cells. All experiments were approved by the Institutional Animal Care and Use Committee of the University of Chicago.

Cell lines

B16-F10 (B16) mouse melanoma cells were purchased from the American Type Culture Collection, OVA-expressing B16-F10 (B16-OVA) were a gift from B. Huard (University of Geneva, Switzerland), and the $Braf^{V600E}/Pten^{-/-}$ cell line (BP) was a gift from T. Gajewski (University of Chicago, USA). B16 and B16-OVA cell lines were maintained in high-glucose Dulbecco's modified Eagle's medium (DMEM) supplemented with 10% heat-inactivated fetal bovine serum (FBS) (both from Invitrogen). BP cell lines were maintained in DMEM high glucose supplemented with 10% FBS and 1% nonessential amino acids (HyClone). VEGF-C–overexpressing and control cell lines were generated by lentiviral transduction of parental cell lines using pD2109-EFs_mVEGF-C and pD2109-EFs empty vector, respectively (ATUM, Newark, CA), and transduced cells were selected on the basis of expression of puromycin resistance. All cell lines used in this study produced between 2.5 and 10 ng of VEGF-C per 10^6 cells over 24 hours of in vitro culture, as measured using a human VEGF-C enzyme-linked immunosorbent assay (ELISA) kit [which is cross-reactive with mouse VEGF-C (R&D Systems, cat. DY752B)]. To generate GM-CSF–overexpressing B16, the parental B16 cell line was transduced with pLVCAG-CMV_mGM-CSF lentivector, generated by cloning mouse GM-CSF coding sequence into the pLVCAG-CMV backbone (Addgene). Individual GM-CSF–overexpressing single-cell clones were isolated by limiting dilution, and a GM-CSF–overexpressing monoclonal cell line with optimal GM-CSF expression (*45*) (average 60 ng GM-CSF/10^6 cells/24 hours, corresponding to 240 ng of GM-CSF per vaccine dose) was used.

Vaccination protocols

Tumor cells were detached with Accutase (Innovative Cell Technologies Inc.), washed, resuspended in high-glucose DMEM supplemented with 10% FBS in a T75 cell culture flask, and immediately irradiated with a 50-Gy x-ray dose using a Philips 250-kVp x-ray unit. Soon after irradiation, cells were washed twice with FBS-free medium and injected intradermally in a shaved area of back skin, close to the right shoulder, at a dose of 4×10^6 cells per mouse in 50 μl. On days 4, 6, 8, and 10 (unless otherwise indicated), 25 mg of 5% IMQ cream (Meda, Solna, Sweden) was applied topically on the cell injection site and gently rubbed until complete absorption. On days 8 and 10, anti-CD40 agonistic antibody variant, engineered to bind extracellular matrix [PlGF-αCD40, described in (*21*) and generated in-house], was injected intradermally at a dose of 30 μg in 40 μl of phosphate-buffered saline (PBS) in the same site. Mice receiving GVAX were vaccinated with 4×10^6 irradiated B16-GM-CSF only, while mice vaccinated with GVAX + adjuvants also received administration of IMQ and PlGF-αCD40 as described above. For VEGFR-3 blockade studies, mice received intraperitoneal injections of 500 μg of anti-VEGFR-3 antibody (mF4-31C1; Eli Lilly) or isotype rat IgG (I4131; Sigma-Aldrich) every 3 to 4 days starting the day of irradiated B16-VEGFC injection. In vaccination experiments involving blockade of sphingosine-1-phosphate (S1P) receptor, the inhibitor FTY720 (Sigma-Aldrich) was injected intraperitoneally daily at 1 mg/kg. For therapeutic tumor vaccination, mice additionally received anti–PD-1 (RMP1-14; BioXCell), injected intraperitoneally on days 6, 9, 13, and 17 at 200 μg per dose.

Tumor experiments

Cultured tumor cells were detached with trypsin (Invitrogen), spun down, and resuspended in serum-free medium to 5×10^6 cells/ml and injected (2.5×10^5 cells in 50 μl) on the left side of the back, approximately equidistant from the front and hind legs. Tumor size was measured with a digital caliper, volume (V) was calculated as $V = 1/6\,\pi \times \text{length} \times \text{width} \times \text{height}$, and mice were euthanized when tumors reached the end point tumor size (500 mm^3) or became ulcerated.

Tissue processing for ex vivo antigen-stimulation and flow cytometry

Spleens and LNs were smashed, filtered through a 70-μm mesh filter and centrifuged at 1500 rpm for 5 min. Red blood cells were lysed with 4 ml of ACK solution (Gibco) for 3 min. Following the addition of cell culture medium, splenocytes were washed and resuspended in IMDM supplemented with 10% FBS, 1% penicillin-streptomycin, and 20 μm 2-β-mercaptoethanol. For experiments involving detection of fluorescent bead uptake by APC subsets in the LNs, LNs were fragmented with syringe needles and digested in collagenase IV (1 mg/ml; Worthington-Biochem) and deoxyribonuclease I (DNAse I) (40 μg/ml; Roche) for 30 min at 37°C with stirring. Supernatants were then carefully collected, and remaining fragments were further digested with Collagenase D (3.3 mg/ml; Roche) and DNAse I (40 μg/ml) for 15 min followed by EDTA addition at a 5 mM final concentration. Tumor and skin samples were cut into small pieces with scissors (tumors) or surgical scalpels (skin) and digested with Collagenase IV (1 mg/ml) and DNAse (40 μg/ml) (tumor) or DNAse I (10 μg/ml) (skin) for 1 hour at 37°C under magnetic stirring. Samples were mixed with an automatic pipette 100 times, the digested cell suspension was collected, and the remaining undigested fragments were incubated with Collagenase D (3.3 mg/ml) and DNAse (40 μg/ml) (tumor) or DNAse (10 μg/ml) (skin) I for 30 min with additional two cycles of repeated pipetting. At the end of the second digestion step, EDTA was added to a final concentration of 5 mM to stop the enzymatic reaction. Cell suspensions from both digestion steps were pooled and filtered through 70-μm cell filters. For tumors, red blood cells (RBCs) were lysed with 1 ml of ACK solution for 1 min. At the end of the digestion protocol, all samples were washed and resuspended in cell culture medium.

For blood collection, approximately 50 μl blood was collected from the saphenous vein into EDTA-K2–coated tubes (Eppendorf), washed with PBS, and centrifuged at 1500 rpm for 5 min. RBCs

were lysed twice with 2 ml of ACK solution for 2 min, each time immediately followed by the addition of PBS supplemented with 2% FBS, centrifugation, and further wash in PBS with 2% FBS.

Adoptive transfer of OT-1 and pmel CD8$^+$ T cells

Spleens and LNs were harvested from OT-1 mice and pmel mice and separately processed as described above. Naïve CD8$^+$ T cells were isolated by negative magnetic cell sorting using EasySep Mouse CD8$^+$ T Cell Isolation Kit (cat. 19853, STEMCELL Technologies) and subsequently labeled with 1 μm CFSE (eBioscience) or CellTrace Violet (Invitrogen) according to the manufacturer's instruction. Mice received an intravenous injection of 2×10^6 OT-1 CD8$^+$ T cells and 1×10^6 pmel CD8$^+$ T cells in 200 μl of serum-free cell culture medium.

Ex vivo antigen stimulation

For evaluation of antigen-specific T cell response induced by B16-based vaccines, splenocytes from vaccinated mice were cocultured with peptide-pulsed bone marrow–derived DCs [BMDCs; isolated according to Lutz *et al.* (*46*)], and cytokine secretion was assessed by enzyme-linked immunosorbent spot (ELISPOT) or ELISA. Briefly, BMDCs were pulsed overnight with 2 μg/ml of antigenic peptides and 0.1 μm CpG to induce DC maturation. Next, BMDCs were washed and incubated with splenocytes at a 10:1 leukocyte:DC ratio in either ELISPOT plates for 20 hours or in u-bottom cell culture plates for 48 hours (for ELISA assessment on cell culture supernatants). Each peptide (1 μg/ml) was added again to the final splenocyte-DC coculture to further boost antigen presentation. The following peptides were used for stimulation: H-2K^b–restricted epitope mTrp2$_{180–188}$ (SVYDFFVWL), H-2D^b–restricted epitope hgp100$_{25–33}$ (KVPRNQDWL), and Kif18b^{mut} and Cpsf3l^{mut} long peptides [27 amino acid–long peptides with the mutated amino acid in position 14, as originally reported (*24*)]. The presence of the described immunogenic non-synonimus point mutations in the Kif18b and Cpsfl3 genes (*24*) in all B16 cell lines used in this study was confirmed by genomic DNA sequencing. Antigen presentation by BMDCs was used in experiments with the B16 model to allow efficient uptake and processing of the Kif18b^{mut} and Cpsf3l^{mut} long peptides. For experiments with BP-based vaccines, because no long peptide was used, splenocytes or LN cells were directly cultured in the presence of either soluble short peptides (mTrp2$_{180–188}$ or hgp100$_{25–33}$, as above, at 1 μg/ml) or irradiated BP parental cells at a 10:1 leukocyte:tumor cell ratio.

Frequencies of IFN-γ–producing splenocytes were assessed using ELISPOT (cat. 551083, BD Biosciences) and reported as either total IFN-γ spots or antigen-specific IFN-γ spots, the latter calculated by subtracting the average spot count in unstimulated control wells to the average spot count in antigen-stimulated wells for each mouse. Cell culture supernatants were assayed by ELISA for IFN-γ and IL-2 (cat. 88-7314-88 and 88-7024-88, respectively, both from Invitrogen).

Flow cytometry

Single-cell suspensions were first stained with Fixable Viability Dye eFluor 455UV (cat. 65-0868-14, eBioscience) and anti-CD16/32 Fc receptor blocking antibody (clone 93, BioLegend) in PBS for 15 min at 4°C. Staining of surface antigens was performed in PBS + 2% FBS for 20 min at 4°C. Following staining, cells were fixed with 2% paraformaldehyde in PBS for 20 min at 4°C, and data were acquired using a LSRFortessa cytometer (BD). For surface staining, the following antibodies were used: CD45 APC-Cy7 (clone 30-F11, BioLegend), CD3 BUV395 (clone 145-2C11, BD Biosciences), CD4 BV785 (clone RM4-5, BioLegend), CD8a Pacific Blue or PE-Cy7 or APC (clone 53-6.7, BioLegend), CD62L PE-Cy7 (clone MEL-14, BioLegend), CD44 PerCP-Cy5.5 (clone IM7, BioLegend or BD Biosciences), CD31 APC or BUV737 (clone MEC 13.3, BD Biosciences), Podoplanin (gp38) PE or APC-Cy7 (clone 8.1.1, BioLegend), CD11b BV786 or BV605 (clone M1/70, BioLegend), Ly-6C BV605 (clone HK1.4, BioLegend), I-A/I-E (MHC-II) PerCP-Cy5.5 (clone M5/114, BD Biosciences or BioLegend), F4/80 APC or FITC (clone Cl:A3-1, BIO-RAD), CD103 PE (Clone M290, BD Biosciences), CD11c BV421 (clone N418, BioLegend), CD45.1 PE (clone A20, BioLegend), and BV605 CD90.1 (Thy-1.1) (clone OX-7, BioLegend). Staining of Trp2-specific CD8$^+$ T cells was performed using R-PE–labeled Pro5 MHC Pentamer H-2Kb SVYDFFVWL (Proimmune, Oxford, UK) according to the manufacturer's instructions.

Immunohistochemistry

Skin samples were fixed with Zinc Fixative (BD Biosciences) for 24 hours at 4°C and subsequently dehydrated by incubation in 20% sucrose for 2 days followed by 30% sucrose for 2 days. Dehydrated tissues were embedded in Tissue-Tek OCT Compound (Electron Microscopy Sciences), slowly frozen on liquid nitrogen vapors, and cut into 8-μm sections using a cryostat (Thermo Fisher Scientific). For immunostaining, sections were incubated for 30 min at room temperature with tris-buffered saline (TBS) + 0.5% Casein to block nonspecific binding sites and then incubated overnight at 4°C with primary antibodies diluted in TBS + 0.5% casein. Following primary antibody staining, sections were washed three times with TBS+ 0.1% Tween 20 and two times in TBS and incubated with fluorochrome-conjugated secondary antibodies diluted in TBS + 0.5% Casein for 3 hours at RT. Secondary antibodies were washed with TBS + 0.1% Tween 20 three times and once with TBS, and slides were mounted with ProLong Gold Antifade Reagent either with or without DAPI (4′,6-diamidino-2-phenylindole) (Invitrogen). Immunostaining was performed using the following primary antibodies: Alexa Fluor (AF) 488 rat anti–Lyve-1 (clone ALY7, eBioscience) and purified rabbit anti-CD3ε (clone SP7, Abcam). Lyve-1 staining signal was further amplified using an anti-rat secondary antibody conjugated to AF488. An anti-rabbit secondary antibody conjugated with either AF594 or AF647 was used in combination with anti-CD3ε primary antibody. Samples were imaged using an Olympus IX83 microscope and images were processed using ImageJ (National Institutes of Health).

Quantitative RT-PCR

Total RNA from tumor cell lines cultured in vitro was extracted using the RNeasy Plus Mini Kit (Qiagen), and retrotranscription was performed using GoScript Reverse Transcriptase transcription kit (Promega) according to the manufacturer's instructions. Quantitative reverse transcription polymerase chain reaction (RT-PCR) was performed using SYBR Green mix and a LightCycler 96 instrument (both Roche). Primer sequences were as follows: gp100, 5′-GAAGGATC-CAGGAATCAGGACTGGCTTG-3′ (forward) and 5′-GCAGTT AGACCCCTGCACCTCTGTC-3′ (reverse); Trp1, 5′-AGTTTC-CACGAGAGTGTGCCAATATTGAGGCTC-3′ (forward) and 5′-GTCGGGAGTCTGCAATCACAGCCAC-3′ (reverse); Trp2, 5′-CAGATCGCCAACTGCAGCGTGTATGAC-3′ (forward) and 5′-ATGGCCTTATAGGGGCGTCCTGGAC-3′ (reverse); β-actin, 5′-TGGAATCCTGTGGCATCCATGAAAC-3′ (forward) and 5′-TAAAACGCAGCTCAGTAACAGTCCG-3′ (reverse). Relative

quantification was calculated with the ΔΔCt method and expressed as $2^{-\Delta\Delta Ct}$. Ct values were normalized first to the endogenous control (β-actin) to obtain the ΔCt and then to the B16-VEGFC samples to obtain the ΔΔCt.

Protein lysate analysis

Skin tissue was snap frozen in liquid nitrogen, and protein lysates were obtained using Tissue Protein Extract Reagent and Halt Protease and Phosphatase Inhibition Cocktail (Thermo Fisher Scientific). After homogenization, lysates were spun down for 10 min at 4°C and 14,000*g*. The supernatants were collected, and protein content was quantified using a bicinchoninic acid assay (BCA assay, Thermo Fisher Scientific). Normalized samples were then analyzed for CCL21 content by ELISA (cat. DY457, R&D Systems).

In vivo toxicity assessment

For toxicity parameter measurements, mouse blood was collected 4 days after completion of the vaccination protocol and allowed to clot for 3 hours at 4°C. The serum was next collected by centrifugation at 2000*g* for 10 min and used for quantification of alanine aminotransferase (ALT), amylase, calcium, creatinine kinase, total bilirubin, and total protein concentration using a Vet Axcel blood chemistry analyzer (Alfa Wasserman).

Statistical analysis

Statistical analysis was performed with Prism (v. 8.2.0, GraphPad, San Diego, CA). Groups were first compared with *F* test to test the hypothesis of equal variances. In the presence of significantly different variances, datasets were compared using either a nonparametric test (specifically Mann-Whitney test for comparison of two groups and Kruskal-Wallis test with Dunn's multiple comparisons post hoc test for comparison of three or more groups) or one-way analysis of variance (ANOVA) with Welch's correction for unequal variances and Dunnett's T3 multiple comparisons. In the presence of equal variances, parametric tests were used, specifically unpaired two-tailed Student's *t* test for comparison of two groups, one-way ANOVA with Tukey's multiple comparisons test for comparison of three or more groups, and two-way ANOVA with Sidak's multiple comparisons test for comparison of dataset containing repeated measurements. Two-tailed paired *t* test was also used where stated in the text. Statistical analysis of survival curves was performed with log-rank test. *P* values were reported as follows: $*P < 0.05$, $**P < 0.01$, and $***P < 0.001$.

SUPPLEMENTARY MATERIALS

Supplementary material for this article is available at http://advances.sciencemag.org/cgi/content/full/7/13/eabe4362/DC1

View/request a protocol for this paper from *Bio-protocol*.

REFERENCES AND NOTES

1. S. Hirosue, E. Vokali, V. R. Raghavan, M. Rincon-Restrepo, A. W. Lund, P. Corthésy-Henrioud, F. Capotosti, C. H. Winter, S. Hugues, M. A. Swartz, Steady-state antigen scavenging, cross-presentation, and $CD8^+$ T cell priming: A new role for lymphatic endothelial cells. *J. Immunol.* **192**, 5002–5011 (2014).
2. A. W. Lund, F. V. Duraes, S. Hirosue, V. R. Raghavan, C. Nembrini, S. N. Thomas, A. Issa, S. Hugues, M. A. Swartz, VEGF-C promotes immune tolerance in B16 melanomas and cross-presentation of tumor antigen by lymph node lymphatics. *Cell Rep.* **1**, 191–199 (2012).
3. E. F. Tewalt, J. N. Cohen, S. J. Rouhani, C. J. Guidi, H. Qiao, S. P. Fahl, M. R. Conaway, T. P. Bender, K. S. Tung, A. T. Vella, A. J. Adler, L. Chen, V. H. Engelhard, Lymphatic endothelial cells induce tolerance via PD-L1 and lack of costimulation leading to high-level PD-1 expression on CD8 T cells. *Blood* **120**, 4772–4782 (2012).
4. A. J. Christiansen, L. C. Dieterich, I. Ohs, S. B. Bachmann, R. Bianchi, S. T. Proulx, M. Hollmén, D. Aebischer, M. Detmar, Lymphatic endothelial cells attenuate inflammation via suppression of dendritic cell maturation. *Oncotarget* **7**, 39421–39435 (2016).
5. V. Lukacs-Kornek, D. Malhotra, A. L. Fletcher, S. E. Acton, K. G. Elpek, P. Tayalia, A. Collier, S. J. Turley, Regulated release of nitric oxide by nonhematopoietic stroma controls expansion of the activated T cell pool in lymph nodes. *Nat. Immunol.* **12**, 1096–1104 (2011).
6. M. Nörder, M. G. Gutierrez, S. Zicari, E. Cervi, A. Caruso, C. A. Guzmán, Lymph node-derived lymphatic endothelial cells express functional costimulatory molecules and impair dendritic cell-induced allogenic T-cell proliferation. *FASEB J.* **26**, 2835–2846 (2012).
7. A. Issa, T. X. Le, A. N. Shoushtari, J. D. Shields, M. A. Swartz, Vascular endothelial growth factor-C and C-C chemokine receptor 7 in tumor cell–lymphatic cross-talk promote invasive phenotype. *Cancer Res.* **69**, 349–357 (2009).
8. J. D. Shields, I. C. Kourtis, A. A. Tomei, J. M. Roberts, M. A. Swartz, Induction of lymphoidlike stroma and immune escape by tumors that express the chemokine CCL21. *Science* **328**, 749–752 (2010).
9. A. W. Lund, M. Wagner, M. Fankhauser, E. S. Steinskog, M. A. Broggi, S. Spranger, T. F. Gajewski, K. Alitalo, H. P. Eikesdal, H. Wiig, M. A. Swartz, Lymphatic vessels regulate immune microenvironments in human and murine melanoma. *J. Clin. Invest.* **126**, 3389–3402 (2016).
10. N. Bordry, M. A. S. Broggi, K. de Jonge, K. Schaeuble, P. O. Gannon, P. G. Foukas, E. Danenberg, E. Romano, P. Baumgaertner, M. Fankhauser, N. Wald, L. Cagnon, S. Abed-Maillard, H. M.-E. Hajjami, T. Murray, K. Ioannidou, I. Letovanec, P. Yan, O. Michielin, M. Matter, M. A. Swartz, D. E. Speiser, Lymphatic vessel density is associated with $CD8^+$ T cell infiltration and immunosuppressive factors in human melanoma. *OncoImmunology.* **7**, e1462878 (2018).
11. M. Fankhauser, M. A. S. Broggi, L. Potin, N. Bordry, L. Jeanbart, A. W. Lund, E. Da Costa, S. Hauert, M. Rincon-Restrepo, C. Tremblay, E. Cabello, K. Homicsko, O. Michielin, D. Hanahan, D. E. Speiser, M. A. Swartz, Tumor lymphangiogenesis promotes T cell infiltration and potentiates immunotherapy in melanoma. *Sci. Transl. Med.* **9**, eaal4712 (2017).
12. E. Song, T. Mao, H. Dong, L. S. B. Boisserand, S. Antila, M. Bosenberg, K. Alitalo, J.-L. Thomas, A. Iwasaki, VEGF-C-driven lymphatic drainage enables immunosurveillance of brain tumours. *Nature* **577**, 689–694 (2020).
13. R. H. Farnsworth, M. G. Achen, S. A. Stacker, The evolving role of lymphatics in cancer metastasis. *Curr. Opin. Immunol.* **53**, 64–73 (2018).
14. M. A. Swartz, A. W. Lund, Lymphatic and interstitial flow in the tumour microenvironment: Linking mechanobiology with immunity. *Nat. Rev. Cancer* **12**, 210–219 (2012).
15. S. Spranger, R. Bao, T. F. Gajewski, Melanoma-intrinsic β-catenin signalling prevents anti-tumour immunity. *Nature* **523**, 231–235 (2015).
16. E. W. Roberts, M. L. Broz, M. Binnewies, M. B. Headley, A. E. Nelson, D. M. Wolf, T. Kaisho, D. Bogunovic, N. Bhardwaj, M. F. Krummel, Critical role for $CD103^+/CD141^+$ dendritic cells bearing CCR7 for tumor antigen trafficking and priming of T cell immunity in melanoma. *Cancer Cell* **30**, 324–336 (2016).
17. S. T. Reddy, A. Rehor, H. G. Schmoekel, J. A. Hubbell, M. A. Swartz, In vivo targeting of dendritic cells in lymph nodes with poly(propylene sulfide) nanoparticles. *J. Control. Release* **112**, 26–34 (2006).
18. V. Triacca, E. Güç, W. W. Kilarski, M. Pisano, M. A. Swartz, Transcellular pathways in lymphatic endothelial cells regulate changes in solute transport by fluid stress. *Circ. Res.* **120**, 1440–1452 (2017).
19. J. G. Cyster, S. R. Schwab, Sphingosine-1-phosphate and lymphocyte egress from lymphoid organs. *Annu. Rev. Immunol.* **30**, 69–94 (2012).
20. A. P. Benechet, M. Menon, D. Xu, T. Samji, L. Maher, T. T. Murooka, T. R. Mempel, B. S. Sheridan, F. M. Lemoine, K. M. Khanna, T cell-intrinsic S1PR1 regulates endogenous effector T-cell egress dynamics from lymph nodes during infection. *Proc. Natl. Acad. Sci.* **113**, 2182–2187 (2016).
21. J. Ishihara, A. Ishihara, L. Potin, P. Hosseinchi, K. Fukunaga, M. Damo, T. F. Gajewski, M. A. Swartz, J. A. Hubbell, Improving efficacy and safety of agonistic anti-CD40 antibody through extracellular matrix affinity. *Mol. Cancer Ther.* **17**, 2399–2411 (2018).
22. M. F. Bachmann, A. Oxenius, Interleukin 2: From immunostimulation to immunoregulation and back again. *EMBO Rep.* **8**, 1142–1148 (2007).
23. B. H. Nelson, IL-2, regulatory T cells, and tolerance. *J. Immunol.* **172**, 3983–3988 (2004).
24. J. C. Castle, S. Kreiter, J. Diekmann, M. Löwer, N. van de Roemer, J. de Graaf, A. Selmi, M. Diken, S. Boegel, C. Paret, M. Koslowski, A. N. Kuhn, C. M. Britten, C. Huber, Ö. Türeci, U. Sahin, Exploiting the mutanome for tumor vaccination. *Cancer Res.* **72**, 1081–1091 (2012).
25. G. Dranoff, E. Jaffee, A. Lazenby, P. Golumbek, H. Levitsky, K. Brose, V. Jackson, H. Hamada, D. Pardoll, R. C. Mulligan, Vaccination with irradiated tumor cells engineered to secrete murine granulocyte-macrophage colony-stimulating factor stimulates potent,

specific, and long-lasting anti-tumor immunity. *Proc. Natl. Acad. Sci. U.S.A.* **90**, 3539–3543 (1993).
26. M. A. Curran, W. Montalvo, H. Yagita, J. P. Allison, PD-1 and CTLA-4 combination blockade expands infiltrating T cells and reduces regulatory T and myeloid cells within B16 melanoma tumors. *Proc. Natl. Acad. Sci. U.S.A.* **107**, 4275–4280 (2010).
27. G. Goyal, K. Wong, C. J. Nirschl, N. Souders, D. Neuberg, N. Anandasabapathy, G. Dranoff, PPARγ contributes to immunity induced by cancer cell vaccines that secrete GM-CSF. *Cancer Immunol. Res.* **6**, 723–732 (2018).
28. J. Duraiswamy, K. M. Kaluza, G. J. Freeman, G. Coukos, Dual blockade of PD-1 and CTLA-4 combined with tumor vaccine effectively restores T-cell rejection function in tumors. *Cancer Res.* **73**, 3591–3603 (2013).
29. F. S. Hodi, M. Butler, D. A. Oble, M. V. Seiden, F. G. Haluska, A. Kruse, S. MacRae, M. Nelson, C. Canning, I. Lowy, A. Korman, D. Lautz, S. Russell, M. T. Jaklitsch, N. Ramaiya, T. C. Chen, D. Neuberg, J. P. Allison, M. C. Mihm, G. Dranoff, Immunologic and clinical effects of antibody blockade of cytotoxic T lymphocyte-associated antigen 4 in previously vaccinated cancer patients. *Proc. Natl. Acad. Sci. U.S.A.* **105**, 3005–3010 (2008).
30. J. M. Goldberg, D. E. Fisher, G. D. Demetri, D. Neuberg, S. A. Allsop, C. Fonseca, Y. Nakazaki, D. Nemer, C. P. Raut, S. George, J. A. Morgan, A. J. Wagner, G. J. Freeman, J. Ritz, C. Lezcano, M. Mihm, C. Canning, F. S. Hodi, G. Dranoff, Biologic activity of autologous, granulocyte-macrophage colony-stimulating factor secreting alveolar soft-part sarcoma and clear cell sarcoma vaccines. *Clin. Cancer Res.* **21**, 3178–3186 (2015).
31. U. E. Burkhardt, U. Hainz, K. Stevenson, N. R. Goldstein, M. Pasek, M. Naito, D. Wu, V. T. Ho, A. Alonso, N. N. Hammond, J. Wong, Q. L. Sievers, A. Brusic, S. M. McDonough, W. Zeng, A. Perrin, J. R. Brown, C. M. Canning, J. Koreth, C. Cutler, P. Armand, D. Neuberg, J.-S. Lee, J. H. Antin, R. C. Mulligan, T. Sasada, J. Ritz, R. J. Soiffer, G. Dranoff, E. P. Alyea, C. J. Wu, Autologous CLL cell vaccination early after transplant induces leukemia-specific T cells. *J. Clin. Invest.* **123**, 3756–3765 (2013).
32. W. T. Curry, R. Gorrepati, M. Piesche, T. Sasada, P. Agarwalla, P. S. Jones, E. R. Gerstner, A. J. Golby, T. T. Batchelor, P. Y. Wen, M. C. Mihm, G. Dranoff, Vaccination with irradiated autologous tumor cells mixed with irradiated GM-K562 cells stimulates antitumor immunity and T lymphocyte activation in patients with recurrent malignant glioma. *Clin. Cancer Res.* **22**, 2885–2896 (2016).
33. T. Tsujikawa, T. Crocenzi, J. N. Durham, E. A. Sugar, A. A. Wu, B. Onners, J. M. Nauroth, R. A. Anders, E. J. Fertig, D. A. Laheru, K. Reiss, R. H. Vonderheide, A. H. Ko, M. A. Tempero, G. A. Fisher, M. Considine, L. Danilova, D. G. Brockstedt, L. M. Coussens, E. M. Jaffee, D. T. Le, Evaluation of cyclophosphamide/GVAX pancreas followed by Listeria-mesothelin (CRS-207) with or without nivolumab in patients with pancreatic cancer. *Clin. Cancer Res.* **26**, 3578–3588 (2020).
34. W.-L. Yan, K.-Y. Shen, C.-Y. Tien, Y.-A. Chen, S.-J. Liu, Recent progress in GM-CSF-based cancer immunotherapy. *Immunotherapy* **9**, 347–360 (2017).
35. J. R. Brahmer, C. Lacchetti, B. J. Schneider, M. B. Atkins, K. J. Brassil, J. M. Caterino, I. Chau, M. S. Ernstoff, J. M. Gardner, P. Ginex, S. Hallmeyer, J. H. Chakrabarty, N. B. Leighl, J. S. Mammen, D. F. McDermott, A. Naing, L. J. Nastoupil, T. Phillips, L. D. Porter, I. Puzanov, C. A. Reichner, B. D. Santomasso, C. Seigel, A. Spira, M. E. Suarez-Almazor, Y. Wang, J. S. Weber, J. D. Wolchok, J. A. Thompson; National Comprehensive Cancer Network, Management of immune-related adverse events in patients treated with immune checkpoint inhibitor therapy: American Society of Clinical Oncology Clinical Practice Guideline. *J. Clin. Oncol. Off. J. Am. Soc. Clin. Oncol.* **36**, 1714–1768 (2018).
36. M. Yarchoan, B. A. Johnson III, E. R. Lutz, D. A. Laheru, E. M. Jaffee, Targeting neoantigens to augment antitumour immunity. *Nat. Rev. Cancer* **17**, 209–222 (2017).
37. R. Kuai, L. J. Ochyl, K. S. Bahjat, A. Schwendeman, J. J. Moon, Designer vaccine nanodiscs for personalized cancer immunotherapy. *Nat. Mater.* **16**, 489–496 (2017).
38. E. J. Lipson, W. H. Sharfman, S. Chen, T. L. McMiller, T. S. Pritchard, J. T. Salas, S. Sartorius-Mergenthaler, I. Freed, S. Ravi, H. Wang, B. Luber, J. D. Sproul, J. M. Taube, D. M. Pardoll, S. L. Topalian, Safety and immunologic correlates of melanoma GVAX, a GM-CSF secreting allogeneic melanoma cell vaccine administered in the adjuvant setting. *J. Transl. Med.* **13**, 214 (2015).
39. A. Z. Obradovic, M. C. Dallos, M. L. Zahurak, A. W. Partin, E. M. Schaeffer, A. E. Ross, M. E. Allaf, T. R. Nirschl, D. Liu, C. G. Chapman, T. O'Neal, H. Cao, J. N. Durham, G. Guner, J. A. B.-D. Valle, O. Ertunc, A. M. D. Marzo, E. S. Antonarakis, C. G. Drake, T-cell infiltration and adaptive Treg resistance in response to androgen deprivation with or without vaccination in localized prostate cancer. *Clin. Cancer Res.* **26**, 3182–3192 (2020).
40. A. Anichini, C. Maccalli, R. Mortarini, S. Salvi, A. Mazzocchi, P. Squarcina, M. Herlyn, G. Parmiani, Melanoma cells and normal melanocytes share antigens recognized by HLA-A2-restricted cytotoxic T cell clones from melanoma patients. *J. Exp. Med.* **177**, 989–998 (1993).
41. Y. Kawakami, M. I. Nishimura, N. P. Restifo, S. L. Topalian, B. H. O'Neil, J. Shilyansky, J. R. Yannelli, S. A. Rosenberg, T-cell recognition of human melanoma antigens. *J. Immunother. Emphas. Tumor Immunol.* **14**, 88–93 (1993).
42. S. Pasquali, A. P. T. van der Ploeg, S. Mocellin, J. R. Stretch, J. F. Thompson, R. A. Scolyer, Lymphatic biomarkers in primary melanomas as predictors of regional lymph node metastasis and patient outcomes. *Pigment Cell Melanoma Res.* **26**, 326–337 (2013).
43. G. J. Tsioulias, R. K. Gupta, G. Tisman, E. C. Hsueh, R. Essner, L. A. Wanek, D. L. Morton, Serum TA90 antigen-antibody complex as a surrogate marker for the efficacy of a polyvalent allogeneic whole-cell vaccine (CancerVax) in melanoma. *Ann. Surg. Oncol.* **8**, 198–203 (2001).
44. M. Kwak, N. E. Farrow, A. K. S. Salama, P. J. Mosca, B. A. Hanks, C. L. Slingluff, G. M. Beasley, Updates in adjuvant systemic therapy for melanoma. *J. Surg. Oncol.* **119**, 222–231 (2019).
45. P. Serafini, R. Carbley, K. A. Noonan, G. Tan, V. Bronte, I. Borrello, High-dose granulocyte-macrophage colony-stimulating factor-producing vaccines impair the immune response through the recruitment of myeloid suppressor cells. *Cancer Res.* **64**, 6337–6343 (2004).
46. M. B. Lutz, N. Kukutsch, A. L. Ogilvie, S. Rössner, F. Koch, N. Romani, G. Schuler, An advanced culture method for generating large quantities of highly pure dendritic cells from mouse bone marrow. *J. Immunol. Methods* **223**, 77–92 (1999).

Acknowledgments: We thank B. Pytowski and Eli Lilly for providing the mF4-31C1 antibody, and T. Gajewski for providing the $Braf^{V600E}$/$PTEN^{-/-}$ cell line. We also thank L. Maillat, P. Hosseinchi, and T. Marchell for the helpful discussions. **Funding:** This study was supported by the National Cancer Institute R01 CA219304 (to M.A.S.) **Author contributions:** M.S.S. and M.A.S. conceived of the study, designed and interpreted the experiments, and wrote the manuscript. M.S.S. additionally designed, performed, and analyzed the experiments. N.M. performed the experiments and edited the manuscript. Y.W. and S.H. performed the experiments. P.S.B. generated genetically engineered GM-CSF–overexpressing cell lines and edited the manuscript. J.I. developed and synthesized the PlGF-anti-CD40 antibody. J.A.H. provided guidance and technical expertise. **Competing interests:** M.S.S., P.S.B., J.A.H., and M.A.S. are inventors on a patent application related to this work filed by the University of Chicago (US-2019-00999485-A1, filed 26 October 2018, published 4 April 2019), and J.I. and J.A.H. are inventors on a patent application related to this work filed by the University of Chicago (WO 2018/195386, filed 28 April 2018, published 25 October 2018). The authors declare that they have no other competing interests. **Data and materials availability:** All data needed to evaluate the conclusions in the paper are present in the paper and/or the Supplementary Materials. Anti–VEGFR-3–blocking antibodies (mF4-31C1) were obtained from Eli Lilly under a material transfer agreement with the University of Chicago (PCT/US2018/28505). Additional data related to this paper may be requested from the authors.

Submitted 21 August 2020
Accepted 22 January 2021
Published 24 March 2021
10.1126/sciadv.abe4362

Citation: M. S. Sasso, N. Mitrousis, Y. Wang, P. S. Briquez, S. Hauert, J. Ishihara, J. A. Hubbell, M. A. Swartz, Lymphangiogenesis-inducing vaccines elicit potent and long-lasting T cell immunity against melanomas. *Sci. Adv.* **7**, eabe4362 (2021).